Surface-Induced Anisotropic Chain Ordering of Polycarprolactone on Oriented Polyethylene Substrate: Epitaxy and Soft Epitaxy

Chao Yan,[†] Huihui Li,*[,†] Jianming Zhang,[‡] Yukihiro Ozaki,[‡] Deyan Shen,[†] Dadong Yan,[†] An-Chang Shi,[§] and Shouke Yan*[,†]

State Key Laboratory of Polymer Physics and Chemistry, Institute of Chemistry, The Chinese Academy of Sciences, Beijing 100080, P. R. of China; Department of Chemistry, School of Science and Technology, Kwansei-Gakuin University, Gakuen, Sanda 669-1337, Japan; and Department of Physics and Astronomy, McMaster University, Hamilton, Ontario L8S 4M1, Canada

Received May 28, 2006; Revised Manuscript Received September 7, 2006

ABSTRACT: Studies on heteroepitaxy of polymers mostly dealt with the resulting mutual orientation relationship of the involving polymer pairs. The molecular dynamics during the expitaxial crystallization process of a polymer was, however, not concerned so far. To disclose the expitaxial crystallization process of polymers on a molecular scale, the structure evolution of polycarprolactone (PCL) in the molten state on highly oriented polyethylene (PE) substrate was followed by time-resolved Fourier transform infrared spectroscopy and wide-angle X-ray diffraction (WAXD). The results clearly indicate the existence of surface-induced anisotropic chain ordering of PCL in its molten state on highly oriented PE substrate, i.e., the occurrence of soft epitaxy. These ordered PCL chain segments in turn initiate the epitaxial crystallization of PCL on highly oriented PE substrate during the subsequent cooling process.

1. Introduction

Heteroepitaxy of polymers has been extensively studied for it provides a useful way to control the crystalline structure, e.g., chain orientation and crystalline modification, of a wide variety of semicrystalline polymeric materials.[1−7] Great progress on understanding its mechanism at a molecular level has been achieved.[8,9] For example, the epitaxial crystallization of polyethylene on highly oriented isotactic polypropylene has been explained in terms of the parallel alignment of PE chains along its crystallographic *b*-axis direction onto the oblique methyl group rows in the lateral *ac* contact plane of iPP with a 0.5 nm intermolecular distance for a chain-row matching.[9] It should be pointed out that, in almost all of the studies on polymer epitaxy, attention has solely been paid to the characterization of the resulting mutual orientation relationship of the involving polymer pairs via atomic force microscopy, X-ray scattering, and transmission electron microscopy combined with electron diffraction. The molecular dynamics during the expitaxial crystallization process of a polymer was, however, not concerned so far. For example, the epitaxial crystallization of PE on highly oriented iPP substrate has been clearly explained in terms of a chain-row matching. But how the PE chains well aligned on the iPP substrate with both polymer chains ±50° apart during the cooling process from random coiled melt is not clear at all. Therefore, a detailed study on the molecular dynamics of a polymer epitaxially crystallizes on another polymer substrate is clearly warranted.

Fourier transform infrared spectroscopy (FTIR) is sensitive to both chain conformation and local molecular environment of a polymer.[10] It has been proved to be a powerful tool for time-resolving not only the molecular structure but also the conformational ordering of semicrystalline polymers.[11−17] In contrast to the above-mentioned techniques for epitaxial structure characterization, by following the chain conformational changes and chain alignment of the deposit polymer, FTIR enables us to in situ study the epitaxial phenomenon at the molecular level in the very early stage or even in a supercooled melt. Therefore, the crystallization process of PCL and its molecular dynamics in the supercooled state on highly oriented PE substrate were in situ followed by electron microscopy, Fourier transform infrared spectroscopy (FTIR), and wide-angle X-ray diffraction (WAXD). The results have not only disclosed the epitaxial process of PCL on PE substrate but also may shed more light on the molecular dynamics of a polymer on an anisotropic substrate.

The purpose of this paper is to present the detailed experimental procedure for following the conformational and ordering change of PCL chains on the PE substrate and some interesting results regarding the molecular dynamics of PCL chains in the molten state on a highly oriented PE substrate.

2. Experimental Section

PE used in this study is Lupolen 6021DX, produced by BASF AG Ludwigshafen, Germany. Commercial grade PCL, with molecular weight $M_w = 65\,000$, polydispersity of 1.53, and melting point of 60 °C, was purchased from Sigma-Aldrich Co. The PE was processed into highly oriented structure through a melt-drawing technique introduced by Petermann and Gohil.[18] The thickness of the resulting PE ultrathin film ranges from 30 to 50 nm. To check the epitaxial behavior of PCL with PE, a double-layered sample was prepared by transferring a thin layer of PCL onto the highly oriented PE substrate. Thus, the prepared sample was heat-treated at 85 °C (below the melting point of PE but above that of PCL) for 15 min and then cooled to 50 °C for isothermal crystallization. After the heat treatment, the sample was observed on a Philips CM200 TEM operated at 200 kV. Phase contrast bright-field (BF) micrographs were obtained by defocus of the objective lens.[19−21] To minimize radiation damage by the electron beam, focusing was carried out on an area; then the specimen film was translated to its adjacent undamaged area, and the image was recorded immediately.

To monitor the molecular dynamics of PCL chains on highly oriented PE substrates, a solution-cast PCL thin film of about 10

[†] The Chinese Academy of Sciences.
[‡] Kwansei-Gakuin University.
[§] McMaster University.

10.1021/ma061188v CCC: $33.50
Published on Web 10/17/2006

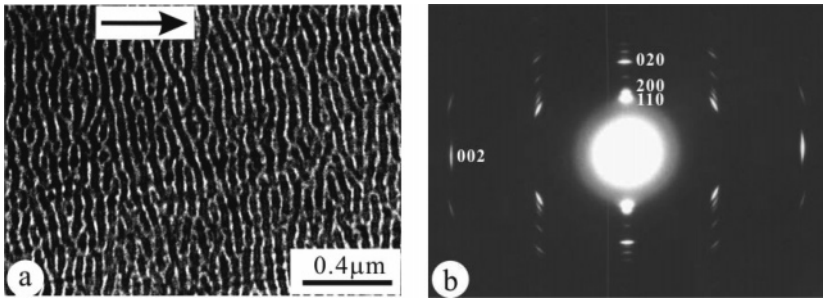

Figure 1. (a) BF electron micrograph and (b) the corresponding electron diffraction pattern of melt-drawn PE thin films.

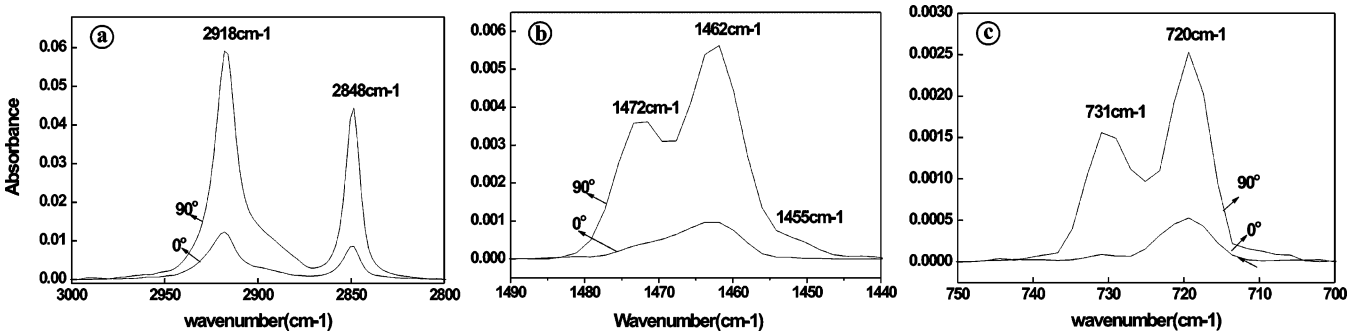

Figure 2. Polarized TIR spectra of melt-drawn PE thin films in different regions.

μm in thickness was sandwiched between two highly oriented ultrathin PE films with the same chain orientation. Such configuration could enhance their contact areas as well as avoid dewetting of the PCL on PE surface.

For FTIR experiments, a Bruker EQUINOX 55 spectrometer equipped with a Bruker P/N 21525 series variable temperature cell was used. The sample was first heated to 85 °C (below the melting point of PE but above that of PCL) for 15 min and then cooled to the required temperature for FTIR measurement. FTIR spectra were in situ recorded at a 2 min interval. Since it was difficult to calculate the integrated intensity precisely due to peak overlaps, the peak height was chosen for data analysis using OPUS software. To testify the mutual chain orientation relationship between PCL and PE substrate, polarized IR spectroscopy measurements with polarized beam parallel and perpendicular to the PE chain direction were conducted. During the experimental process, the sample was protected with dry N_2.

WAXD experiments were carried out using a 12 kW rotating-anode generator (Cu KR) in combination with a Geigerflex D/max-RB diffractometer. The reflection peak positions and widths were calibrated with silicon powder ($2\theta > 15°$) and silver behenate ($2\theta < 10°$). Powder patterns were taken in reflection mode at a scan rate of 10°/min within the 2θ angle region of 10°−35°. During all of the experimental process, the sample was protected with dry N_2.

3. Results and Discussion

Structure of Melt-Drawn PE Substrate Film. For a better understanding, the structural feature of the used PE substrate film was first presented. Figure 1 shows the BF electron micrograph and corresponding electron diffraction of the melt-drawn PE thin films. The arrow in the picture indicates its drawing direction during sample preparation. In the defocused phase contrast BF images, the bright lines represent the lower mean inner potential amorphous regions, while the gray areas between the bright lines are the high-density crystalline lamellar regions. From the BF image Figure 1a, it can be clearly seen that the melt-drawn PE film consists of edge-on lamellae aligned perpendicular to the drawing direction, indicating a high degree of crystal orientation. On the corresponding electron diffraction pattern, Figure 1b, the appearance of sharp and well-defined reflection spots confirms that the PE melt-drawn films are highly oriented. The alignment of the (002) diffraction spots along the drawing direction of the sample reflects an orientation with the chain axis in the film plane and along the drawing direction. Furthermore, on the meridian direction of the diffraction pattern, the coexistence of the (200), (020), and many other (*hk*0) reflection spots indicates a high degree of fiber orientation with the crystallographic *c*-axis parallel to the drawing direction and the crystallographic *a*- and *b*-axes rotating randomly around the *c*-axis.[22]

Polarized infrared spectroscopy was also used to characterize the structure of the oriented PE thin film. The infrared spectroscopic features of PE were well-known based on many detailed studies.[23−25] It was reported that the doublet 731 and 720 cm^{-1} bands originated from a factor group splitting due to the intermolecular interaction of the CH_2 sequences packed in an orthorhombic unit cell. Similar behavior has been found for the CH_2 bending bands at 1472 and 1462 cm^{-1}. Consequently, these bands were chosen to characterize the orientation in crystalline phase. The vibration directions of these bands are all perpendicular to the chain skeleton axis. Considering that the bands at 2918 and 2848 cm^{-1} represent the total asymmetric and symmetric CH_2 stretching vibrations of the molecular chains and exhibit perpendicular transition moments with respect to the main chain of PE, they were chosen as characteristic bands for overall orientation degree measurements. Figure 2 shows the TIR spectra of these bands with the electron vector perpendicular "⊥" and parallel "∥" to the drawing direction of the PE thin film. The difference between the TIR spectra with the electron vector perpendicular "⊥" and parallel "∥" to the drawing direction of the PE thin film is quite clear. The absorption intensities for the perpendicular polarization (indicated as 90° in the figures) are much higher than that for the parallel polarization (described as 0°) of these bands. This demonstrates a parallel alignment of the PE chains along the drawing direction since all of these bands have perpendicular transition moments with respect to the main chain. The extent of chain orientation is usually described by an orientation

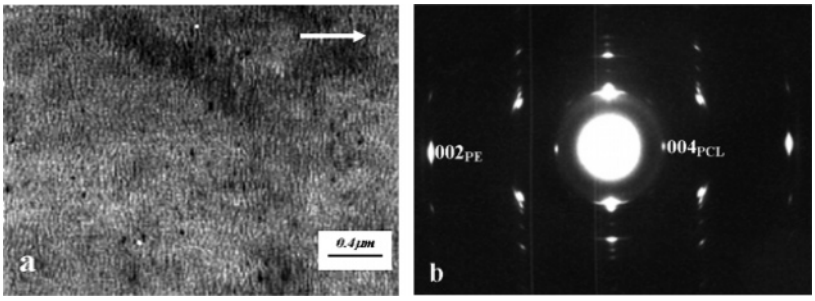

Figure 3. (a) BF electron micrograph and (b) the corresponding electron diffraction pattern of a PCL/PE double-layered thin film heat-treated at 80 °C for 10 min and subsequently crystallized isothermally at 50 °C for 24 h.

Table 1. Orientation Function of Characteristic Infrared Bands of PE Substrate Film

bands (cm^{-1})	orientation function (f)	bands (cm^{-1})	orientation function (f)
2918	0.717 48	1472	0.833 22
2848	0.736 66	731	0.915 89
1462	0.764 32	720	0.715 56

function f defined as[26]

$$f = \frac{R-1}{R+2}\frac{2}{3\cos^2\alpha - 1}$$

where α is the angle between the chain axis and the transition moment associated with the infrared band used for the measurement; R is the measurable infrared dichroic ratio defined as $R = A_{\parallel}/A_{\perp}$, with $A_{\parallel}$ and $A_{\perp}$ reflecting the absorbance when the infrared beam was polarized parallel and perpendicular to the chain direction, respectively. In the present case, considering that all of the chosen bands exhibit perpendicular transition moments with respect to the main chain, the f corresponding to each band can be calculated taking $\alpha = 90°$. As summarized in Table 1, the f value of 0.7−0.9 for all of the chosen bands indicates a high degree of PE chain orientation in both crystalline and amorphous phases. It should be pointed out that overlapping of the amorphous band at 723 cm^{-1} with the crystalline one at 720 cm^{-1} may result in a decrease of the f value for the 720 cm^{-1} band. The same situation may happen for the 1462 cm^{-1} band (probably also some extent to the 1472 cm^{-1} band), which overlaps with the amorphous bands at 1467 and 1455 cm^{-1}. Nevertheless, the f value indicates a high degree of chain orientation of PE, especially in the crystalline phase.

Epitaxial Crystallization of PCL on Highly Oriented PE Substrate. Figure 3 shows the BF electron micrograph and its corresponding electron diffraction pattern of a PCL/PE double-layered film, which was heat-treated at 85 °C for 15 min and subsequently crystallized isothermally at 50 °C for 24 h. The arrow in the picture indicates the molecular chain direction of PE substrate. Clearly, an oriented structure of PCL arises with its crystalline lamellae perpendicular to the chain direction of PE substrate (Figure 3a). This indicates the occurrence of epitaxial crystallization of PCL on the PE substrate.[27,28] The electron diffraction result (Figure 3b) further confirms that the PCL grows epitaxially on the PE substrate with the molecular chains aligned exactly parallel to the chain direction of PE substrate. For the above-observed results, a most frequently asked and well-understood question is regarding the origin of the unusual parallel alignment of PCL on PE substrate. This can be explained in terms of geometric matching. On the basis of the almost identical orthorhombic unit cells of PCL with parameters $a = 0.747$, $b = 0.498$, and $c = 1.705$ nm and PE with parameters $a = 0.74$, $b = 0.494$, and $c = 0.253$ nm, perfect matching can be found between every *(hk*0) pair. For example, the mismatching between the (010) lattice planes of both polymers is only 0.8%, while that between the (100) lattice planes is ca. 0.9%. Moreover, the 0.122 nm interatomic space along chain axis of PCL matches that of PE, 0.123 nm, also very well.[28] Therefore, the expitaxial crystallization of PCL on PE substrate can be explained in terms of a two-dimensional geometric matching.

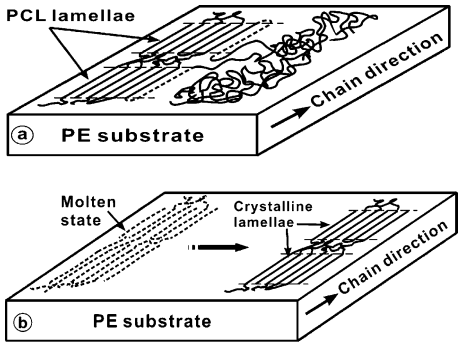

Figure 4. Sketches show the possible chain ordering process of PCL on an oriented PE substrate.

It should be pointed out, however, there exists a less concerned problem regarding how the PCL chains aligned parallel to the chain direction of the PE substrate from the random coiled melt. As sketched in Figure 4, there are two possible ways to realize the parallel alignment of PCL on PE substrate. The first possibility is that the random coiled PCL chain segments aligned parallel to the PE chains while registered on the crystal growth front during crystallization to fulfill the lattice matching (see the dotted lines in Figure 4a). Another possibility is that the PCL chains in the supercooled molten state possess already a roughly parallel alignment with respect to PE chains (see left part of Figure 4b with dotted lines representing the polymer chains in the molten state, which results in a parallel epitaxy during the cooling process as indicated in the right part of Figure 4b). The problem is how to find out the molecular dynamics of this process. For the first possibility, it is clearly impossible to follow the crystallization process on a molecular scale. Therefore, our attention is focused on the second possibility, which can be easily attested through following the conformation and orientation change of the PCL chain in melt or supercooled melt on PE substrate.

Molecular Dynamics of PCL on Highly Oriented PE Substrate. To fulfill the purpose for monitoring the molecular dynamics of the PCL chains in molten state on highly oriented PE substrate, a suitable temperature for ensuring the nonoccurrence of PCL crystallization should be determined first. We here set the temperature at 59 °C (only 1 °C below the measured melting temperature) to prevent the crystallization of PCL. Figure 5a shows the WAXD intensity profiles taking with a

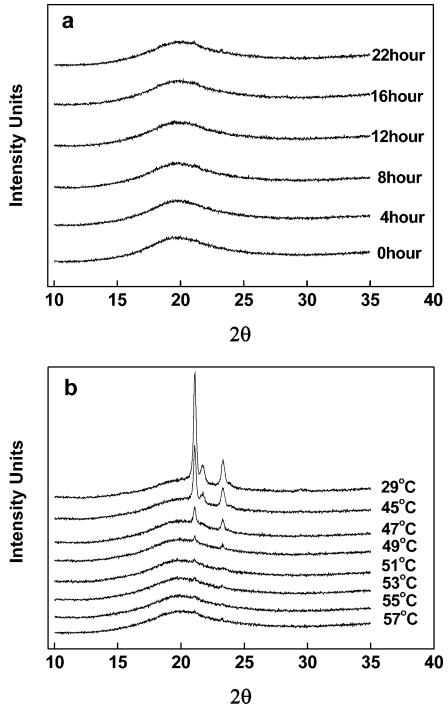

Figure 5. WAXD intensity profile of PCL melt on oriented PE substrate at 59 °C for different time (a) and during the subsequent cooling process (b). The sample was first heat to 85 °C for 10 min to erase the possible thermal history and then cooled direct to 59 °C 22 h. In the cooling process, the sample was stabilized at each temperature for 10 min.

PE/PCL/PE sandwich sample, which was first heated to 85 °C for 15 min and then cooled to and kept at 59 °C for ca. 2 days. Figure 5a shows only an amorphous halo during the whole process. This indicates unambiguously that (i) the PE substrate film is too thin to produce WAXD signal at present conditions and (ii) the crystallization of PCL does indeed not take place at 59 °C for more than 20 h. During the cooling process, one can find that the crystallization of PCL on PE substrate starts actually by cooling the samples down to about 50 °C (see Figure 5b). This was further confirmed by DSC experiments. Therefore, the molecular dynamics of PCL in molten state on highly oriented PE substrate can be followed by infrared spectroscopy at 59 °C.

For infrared spectroscopic characterization, correct band assignments of PCL are the essential requirement for a reasonable analysis. The band assignments given in the literature are summarized in Table 2.[29−31] Taking into account that the PCL has an almost identical crystal structure as the PE crystal, especially for the *a* and *b* unit cell dimensions,[32,33] the731 and 710 cm^{-1} bands should be originated from a factor group splitting due to the intermolecular interaction of the CH_2 sequences packed in an orthorhombic unit cell just as in the case of PE crystals. It was confirmed that by melting the PCL sample the 710 cm^{-1} band completely disappeared, while the

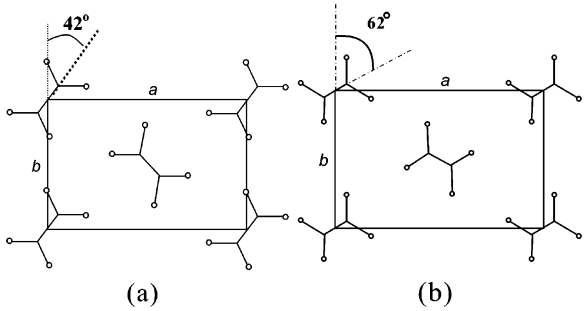

Figure 6. Sketches show the unit cells of (a) PE and (b) PCL in the *ab* projection.

731 cm^{-1} peak was reduced to about one-third its original height. This further indicates that these two bands are primarily the crystalline peaks. Moreover, as sketched in Figure 6, a bigger setting angle (defined as the angle between the transplanar C−C chain skeleton and (0*k*0) lattice planes) of PCL, ca. 62°,[32] with respect to that of PE, about 42°,[34] makes approximately a 5% decrease in the distance between the CH_2 groups of the neighboring chains in the PCL unit cell with respect to that in the PE unit cell. This results in a stronger intermolecular interaction of PCL than PE. As a result, a wider splitting of these bands has been seen in PCL crystals than in PE crystals. On the basis of the above analysis, the 731 and 710 cm^{-1} bands were considered to be the crystalline sensitive bands directly related to the three-dimensional ordered structure of PCL, while the rest of the bands were thought to be associated primarily with the specific chain conformation in the crystalline phase. Considering that the 710 cm^{-1} band has relatively very low intensity and small extent of change during crystallization, the conformational sensitive bands at 1295, 1245, and 1192 cm^{-1} and the crystalline sensitive band at 731 cm^{-1} were used for the structure analysis.

To disclose the molecular dynamics of PCL on the oriented PE substrate, the bulk crystallization of PCL from melt was first investigated. The crystallization temperature was set at 50 °C since at higher temperature the crystallization of PCL cannot proceed, while at lower temperature the crystallization of PCL proceeds too fast to be followed. Figure 7 shows the time-dependent spectral evolution during the melt-crystallization process of PCL on KBr at 50 °C. According to the peak assignment mentioned above, the bands in the high wavenumber region, e.g., the 1335−1125 cm^{-1} region of Figure 7a, reflect distinctive chain conformation changes during the isothermal crystallization, while the bands at 710 and 731 cm^{-1} provide principally the formation of three-dimensional ordered crystalline structure, as shown in Figure 7b. From parts a and b of Figure 7, it can be clearly seen that the intensities of both the conformational sensitive bands and crystalline sensitive bands increase with the progress of crystallization. For clarity, the intensity changes of 1295, 1245, 1192, and 731 cm^{-1} bands as a function of crystallization time are plotted in Figure 8a, whereas the corresponding intensity change ratio of these bands,

Table 2. Characteristic Infrared Bands of PCL in the Crystalline Phase

wavenumber	assignments	direction	abbreviation
2944	asymmetric CH_2 stretching	⊥ to the *CC* axis	$\nu_{as}(CH_2)$
2865	symmetric CH_2 stretching	⊥ to the *CC* axis	$\nu_{s}(CH_2)$
1727	carbonyl stretching	intersect the *CC* axis	ν(C═O)
1295	C−O and C−C stretching	∥ to the *CC* axis	ν(C−O C−C)
1245	asymmetric COC stretching	∥ to the *CC* axis	ν_{as}(COC)
1192	OC−O stretching	∥ to the *CC* axis	ν(OC−O)
731	CH_2 rocking in-phase	⊥ to the *CC* axis	$\gamma_{in}(CH_2)$
710	CH_2 rocking out-of-phase	⊥ to the *CC* axis	$\gamma_{out}(CH_2)$

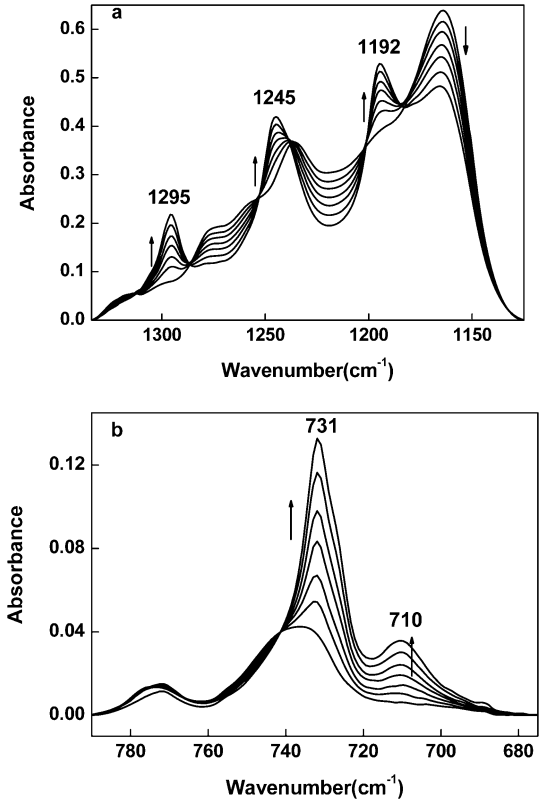

Figure 7. Time-dependent FTIR spectra of PCL crystallized on a KBr plate at 50 °C in wavenumber regions of (a) 1335−1125 and (b) 790−675 cm^{-1}. The arrows indicate the directions of the band intensity changes with crystallization time.

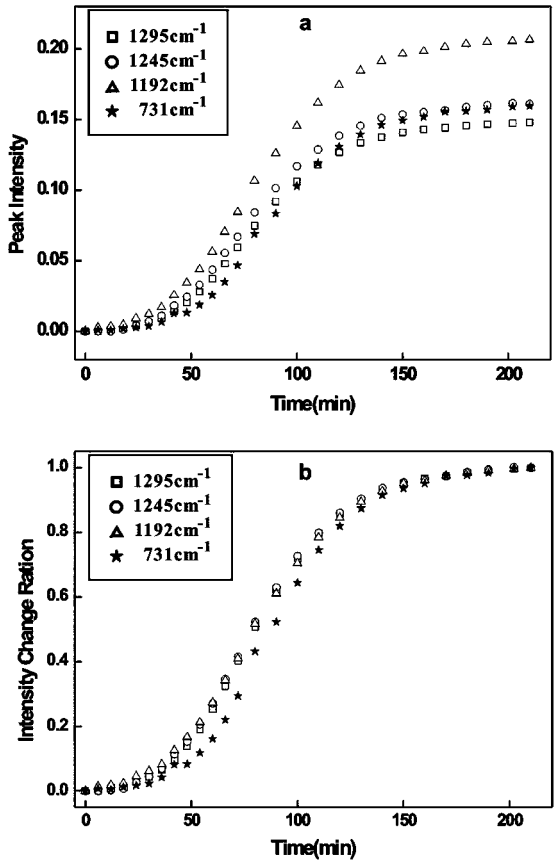

Figure 8. (a) Intensity changes in IR bands at 1295, 1245, 1192, and 731 cm^{-1} as a function of time during the isothermal crystallization of PCL on a KBr plate at 50 °C. (b) Corresponding intensity change ratio vs time.

or in other words the normalized plots of peak intensity vs crystallization time, are presented in Figure 8b. The intensity change ratio is defined as $(H_t - H_0)/(H_\infty - H_0)$ with H_0, H_t, and H_∞ representing the peak height at the crystallization time of zero, t, and the end of isothermal crystallization, respectively. The zero crystallization time is defined as the time at which the temperature of the sample reaches the crystallization temperature, i.e., 50 °C. The intensity of the band at 2865 cm^{-1} was chosen as an internal standard to eliminate the influence of film thickness. From Figure 8, it can be seen that, during the isothermal crystallization process, the intensities of all the characteristic bands at 1295, 1245, 1192, and 731 cm^{-1} increase very slowly in the first 50 min, then significantly in the following 50 min, and finally slowing down before reaching an equilibrium. This may reflect the different crystallization regimes of PCL, i.e., induction period, primary, and secondary crystallization stages. It should be pointed out that there is a small time lag in the intensity change of the 731 cm^{-1} band with respect to that of other bands, as revealed in Figure 8b. This means that the conformational change of PCL chains takes place somewhat prior to the crystallization. That is to say, the PCL chains obtained first the similar conformation as in the crystalline phase and then packed into the crystalline lattice. This phenomenon has also been found in cold crystallization of other polymers, such as isotactic and syndiotactic polystyrene,[35,36] polypropylene,[37,38] poly(bisphenol A-*co*-decane),[39] poly(ethylene terephthalate),[40,41] and poly(ethylene naphthalene),[42] and may be associated with the coupling of density and chain conformation in the supercooled melt prior to polymer crystallization.

Figure 9 shows the time-dependent variations in FTIR spectra of PCL melt on an oriented PE substrate at 59 °C. According to the above-mentioned peak assignment, Figure 9a shows the changes of conformation sensitive bands, while Figure 9b illustrates principally the formation of three-dimensional ordered crystalline structure. It is clear that the intensities of conformational sensitive bands at 1295, 1245, and 1192 cm^{-1} increase with time more quickly than that of crystalline sensitive bands at 731 and 710 cm^{-1}. This can be more clearly seen from the plots of intensity changes of these bands as a function of time, as shown in Figure 10a. The intensity of the 2865 cm^{-1} band was again chosen as an internal standard to eliminate the influence of film thickness. From Figure 10a, we can find that, keeping the PCL melt on oriented PE substrate at 59 °C, the conformational sensitive bands of PCL behave in a similar way as in the case of its crystallization process on the KBr plate at 50 °C (compare Figure 10a with Figure 8a). The intensity change of these conformational sensitive bands is, however, much slower than that on the KBr plate. While the intensity of these bands reaches almost the maximum value in 150 min on KBr plate at 50 °C, 600 min is needed for these bands to get the maximum heights on oriented PE substrate at 59 °C. Moreover, the intensity change of the crystalline sensitive band at 731 cm^{-1} is quite small; especially in the first 200 min, it remains almost unchanged. As shown in Figure 10a, only a slight intensity increase of the 731 cm^{-1} band can be recognized by keeping the sample at 59 °C for long time, e.g., 20 h. The time lag for the intensity increase of the 731 cm^{-1} band can also be clearly identified in the normalized plots of peak intensity vs time presented in Figure 10b. This is clearly different from the case of isothermal crystallization. Furthermore, considering that the 731 cm^{-1} band is the crystalline peak originated from the intermolecular interaction of the CH_2 sequences packed in an orthorhombic unit cell, one may suggest the occurrence of

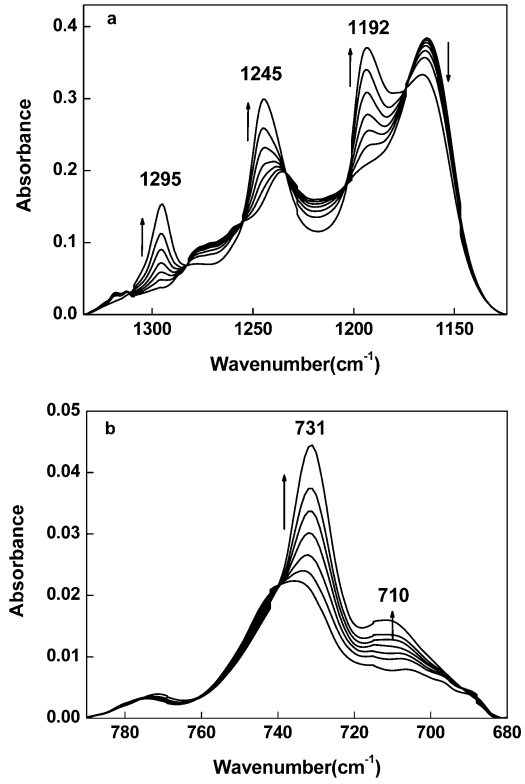

Figure 9. Time-dependent FTIR spectra of PCL kept on an oriented PE substrate at 59 °C from melt in the wavenumber regions of (a) 1335−1125 and (b) 790−675 cm^{-1}. The arrows indicate the directions of band intensity changes with time.

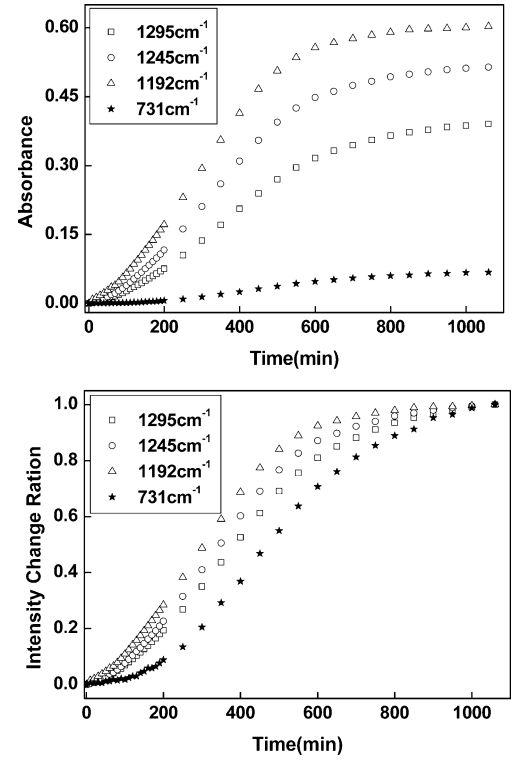

Figure 10. (a) Intensity changes in IR bands at 1295, 1245, 1192, and 731 cm^{-1} as a function of time during the keeping process of PCL on PE substrate at 59 °C. The samples were first heat-treated at 85 °C for 10 min and then cooled to 59 °C. (b) Corresponding intensity change ratio vs time.

crystallization of PCL on PE substrate at 59 °C. This is, however, in contradiction with the WAXD result. A possible explanation of this phenomenon is that some of the short PCL

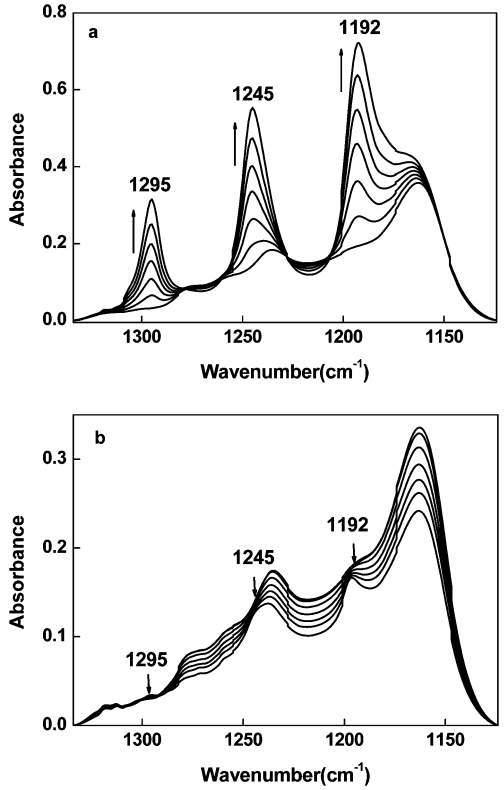

Figure 11. Time-dependent polarized FTIR spectra of PCL melts kept on an oriented PE substrate at 59 °C with polarized beam aligned (a) parallel and (b) perpendicular to the PE chain direction.

chain sequences are aligned in a similar way as in its crystalline phase. These short chain sequences exhibit already the intermolecular interaction, which produces a slight increase in peak intensity of the 731 cm^{-1} band. These interacting chain sequences are not packed in an orthorhombic unit cell at 59 °C but will act as the crystallization precursors, which lead to the subsequent epitaxial crystallization of PCL on the PE substrate during cooling. If this hypothesis is true, these chain sequences should exhibit the same chain orientation as in the final crystalline structure. This becomes an ideal indicator for following the chain arrangement of PCL in melt on PE substrate. To clarify the validity of the above hypothesis, polarized IR spectroscopy measurements were conducted during keeping the PCL melt on PE substrate at 59 °C. Figure 11 shows the time-dependent FTIR spectra of PCL melt on an oriented PE substrate at 59 °C with polarized IR beam aligned parallel and/or perpendicular to the PE chain direction. It is evident that when the polarized infrared beam parallels to the chain direction of PE (see Figure 11a), the absorbance of conformational bands at 1295, 1245, and 1192 cm^{-1} increases significantly with time. On the contrary, as shown in Figure 11b, the IR bands at those positions decrease a little bit with time if the polarized beam is perpendicular to the PE chain backbone. Considering that the transition moments of all these bands are parallel to the chain backbone of PCL, the obtained results indicate that the PCL chains are indeed aligned gradually along the oriented PE chains. This means that the PCL chains in the molten state have already possessed a relative orientation with respect to the PE substrate before crystallization, i.e., the occurrence of soft epitaxy of PCL on highly oriented PE substrate. Similar chain segment ordering prior to crystallization has also been reported in bulk crystallization of polymers.[43,44]

To get more detailed information about the orientation process of the PCL chains, the orientation function *f* of PCL was also

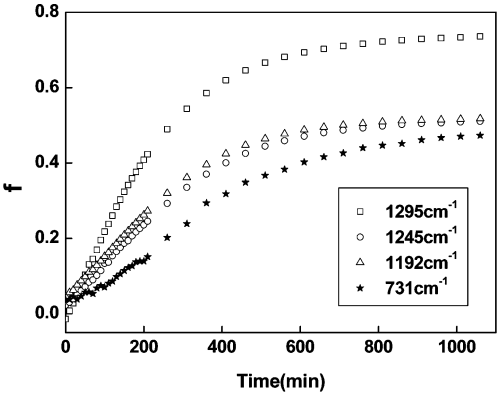

Figure 12. Changes of orientation function *f* vs time for the sample used in Figure 11.

calculated. The variation of *f* for different bands with time is presented in Figure 12. From Figure 12, it can be seen that the PCL chains align quickly along the PE chain direction in the first 400 min and then reach an equilibrium state gradually. Moreover, two things regarding the orientation process should be addressed. First of all, comparing Figure 12 with Figure 10a, one may recognize that the ordering of the PCL chain proceeds more quickly than the change of chain conformation in the first 200 min. This may imply that, keeping the PCL melt on highly oriented PE substrate at 59 °C, the PCL chains first orient gradually along the chain direction of PE crystals due to the strong interaction between PCL and PE, which provides the driving force for the occurrence of heteroepitaxy. The intermolecular interaction of the parallel aligned PCL chains results then in the formation of planar zigzag chain conformation to minimize the free energy of the PCL melt. As a consequence, ordering of the PCL chains in the molecular direction of PE goes more quickly than the chain conformation change at the beginning. With the increase in the amount of parallel aligned PCL chains, more and more PCL chains get the planar zigzag chain conformation via intermolecular interaction. Second, after keeping the PCL on PE substrate at 59 °C for about 20 h, except for the 1295 cm^{-1} band, a value of ca. 0.5 is obtained for the orientation function of each band. This value may indicate that the orientation of PCL chains is poorer than that of PE chains. Combining the fact that PCL crystallizes epitaxially on the PE substrate with both polymer chains exactly parallel (see the electron diffraction pattern shown in Figure 3b), this result may again leads to the conclusion that the crystallization of PCL on PE at 59 °C does not take place. Moreover, the orientation function of the characteristic crystalline 731 cm^{-1} band, ca. 0.47, is the lowest one of the calculated bands. This is different from that of PE oriented substrate, where the *f* for 731 cm^{-1} band has the highest value (ca. 0.9), indicating a better orientation of PE chains in the crystalline state. The lower *f* value of the 731 cm^{-1} band with respect to the conformation sensitive band also supports the nonoccurrence of PCL crystallization. This is in accordance with the WAXD result.

4. Summary

In summary, the structure and structure evolution of PCL on highly oriented PE substrate were successfully followed by electron microscopy, FTIR, and X-ray diffraction. Electron microscopy results clearly indicate that PCL can grow epitaxially on oriented PE substrate with chain axis parallel to the chain direction of PE on the basis of a two-dimensional matching. WAXD results show that no crystallization takes place by keeping the PCL melt on PE substrate at 59 °C for more than 20 h. FTIR measurements illustrate, however, a gradual parallel alignment of the PCL chains along the chain direction of PE during keeping on PE at 59 °C. FTIR further demonstrate that the parallel aligned PCL chains originated from strong mutual interaction between PCL and PE, leading to the formation of planar zigzag chain conformation like in its crystalline phase. This reflects the occurrence of soft epitaxy of PCL on the PE substrate. During the cooling process, the ordered PCL chains should act as the crystallization precusors and initiate the heteroepitaxial crystallization of PCL on PE substrate. This leads to a parallel chain alignment of both polymers. From these results, it is concluded that the heteroepitaxy of PCL on PE substrate takes place through a three-dimensional ordered arrangement of the PCL chains, which are already aligned, more or less, along the PE chain direction in the molten state.

Acknowledgment. The financial support of the Outstanding Youth Fund (No. 20425414), the National Natural Science Foundations of China (No. 50521302, 20574079, 20634050, and 20423003), and the 973 programs from MOST of China is gratefully acknowledged.

References and Notes

(1) Zhang, J.; Yang, D.; Thierry, A.; Wittmann, J. C.; Lotz, B. *Macromolecules* **2001**, *34*, 6261.
(2) (a) Wittmann, J. C.; Lotz, B. *J. Polym. Sci., Polym. Phys. Ed.* **1981**, *19*, 1853; **1981**, *19*, 1837. (b) Wittmann, J. C.; Lotz, B. *J. Polym. Sci., Part B: Polym. Phys.* **1986**, *24*, 1559.
(3) Lotz, B.; Wittmann, J. C. *J. Polym. Sci., Part B: Polym. Phys.* **1987**, *25*, 1079.
(4) (a) Kopp, S.; Wittmann, J. C.; Lotz, B. *Polymer* **1994**, *35*, 908. (b) Kopp, S.; Wittmann, J. C.; Lotz, B. *Polymer* **1994**, *35*, 916.
(5) Lovinger, A. J. *Polymer* **1981**, *22*, 412.
(6) (a) Yan, S. K.; Yang, D.; Petermann, J. *Polymer* **1998**, *39*, 4569. (b) Yan, S. K.; Yang, D.; Petermann, J. *J. Polym. Sci., Polym. Phys.* **1997**, *35*, 1415.
(7) Sun, Y. J.; Li, H. H.; Huang, Y.; Chen, E. Q.; Zhao, L.; Gan, Z. H.; Yan, S. K. M*acromolecules* **2005**, *38*, 2739.
(8) Wittmann, J. C.; Lotz, B. *Prog. Polym. Sci.* **1990**, *15*, 909.
(9) Wittmann, J. C.; Lotz, B. *J. Polym. Sci., Polym. Phys. Ed.* **1985**, *23*, 205.
(10) Esposito, L. D.; Koening, J. L. *J. Polym. Sci., Polym. Phys. Ed.* **1976**, *12*, 1731.
(11) Nakaoki, T.; Yamanaka, T.; Ohira, Y.; Horii, F. *Macromolecules* **2000**, *33*, 2718.
(12) Tashiro, K.; Ueno, Y.; Yoshioka, A.; Kobayashi, M. *Macromolecules* **2001**, *34*, 310.
(13) Wu, H. D.; Tseng, C. R.; Chang, F. C. *Macromolecules* **2001**, *34*, 2992.
(14) Matsuba, G.; Kaji, K.; Nishida, K.; Kanaya, T.; Imai, M. *Macromolecules* **1999**, *32*, 8932.
(15) Jiang, Y.; Gu, Q.; Li, L.; Shen, D. Y.; Jin, X. G.; Chan, C. M. *Polymer* **2003**, *44*, 3509.
(16) Zhang, J. M.; Duan, Y. X.; Shen, D. Y.; Yan, S. K.; Noda, I.; Ozaki, Y. *Macromolecules* **2004**, *37*, 3292.
(17) Duan, Y. X.; Zhang, J. M.; Shen, D. Y.; Yan, S. K. *Macromolecules* **2003**, *36*, 4874.
(18) Petermann, J.; Gohil, R. M. *J. Mater. Sci.* **1979**, *14*, 2260.
(19) Petermann, J.; Gleiter, H. *Philos. Mag.* **1975**, *31*, 929.
(20) Miles, J. M.; Petermann, J. *J. Macromol. Sci., Phys. B* **1979**, *16*, 243.
(21) Thomas, E. L. *Encycl. Polym. Sci. Eng.* **1986**, *5*, 644.
(22) Petermann, J.; Gleiter, H. *Philos. Mag.* **1973**, *28*, 1279.
(23) Synder, R. G. *J. Mol. Spectrosc.* **1961**, *6*, 116.
(24) Hagemann, H.; Snyder, R. G.; Peacock, A. J.; et al. *Macromolecules* **1989**, *22*, 3600.
(25) (a) Tasumi, M.; Shimanouchi, T. *J. Chem. Phys.* **1956**, *25*, 1044. (b) Tasumi, M.; Shimanouchi, T. *J. Chem. Phys.* **1957**, *26*, 1391. (c) Tasumi, M.; Shimanouchi, T. *J. Chem. Phys.* **1965**, *43*, 1245.
(26) Fraser, R. D. B. *J. Chem. Phys.* **1953**, *21*, 1511.
(27) Liu, J. C.; Li, H. H.; Yan, S. K.; Xiao, Q.; Petermann, J. *Colloid Polym. Sci.* **2003**, *281*, 601.
(28) Takahashi, T.; Teraoka, F.; Tsujimoto, I. *J. Macromol. Sci., Phys.* **1976**, *B12*, 303.
(29) Coleman, M. M.; Zarian, J. *J. Polym. Sci., Polym. Phys. Ed.* **1979**, *17*, 837.

(30) Hubble, D.; Cooper, S. *J. Polym. Sci., Polym. Phys. Ed.* **1977**, *15*, 1143.
(31) Elzein, T.; Nasser-Eddine, M.; Delaite, C.; Bistac, S.; Dumas, P. *J. Colloid Interface Sci.* **2004**, *273*, 381.
(32) Bittiger, H.; Marchessault, R. H.; Niegisch, W. D. *Acta Crystallogr.* **1970**, *B23*, 1923.
(33) Chatani, Y.; Okita, Y.; Tadokoro, H.; Yamoshita, Y. *Polym. J.* **1970**, *1*, 555.
(34) Abbate, S.; Gussoni, M.; Zerbi, G. *J. Chem. Phys.* **1979**, *70*, 3577.
(35) Wu, H. D.; Tseng, C. R.; Chang, F. C. *Macromolecules* **2001**, *34*, 2992.
(36) (a) Matsuba, G.; Kaji, K.; Nishida, K.; Kanaya, T.; Imai, M. *Polym. J.* **1999**, *31*, 722. (b) Matsuba, G.; Kaji, K.; Nishida, K.; Kanaya, T.; Imai, M. *Macromolecules* **1999**, *32*, 8932.
(37) Heeley, E. L.; Maidens, A. V.; Olmsted, P. D.; Bras, W.; Dolbnya, I. P.; Fairclough, J. P. A.; Terrill, N. J.; Ryan, A. J. *Macromolecules* **2003**, *36*, 3656.
(38) Terrill, N. J.; Fairclough, P. A.; Towns-Andrews, E.; Komanschek, B. U.; Young, R. J.; Ryan, A. J. *Polymer* **1998**, *39*, 2381.
(39) Jiang, Y.; Gu, Q.; Li, L.; Shen, D. Y.; Jin, X. G.; Chan, C. M. *Polymer* **2003**, *44*, 3509.
(40) Imai, M.; Kaji, K.; Kanaya, T.; Sakai, Y. *Phys. Rev. B* **1995**, *52*, 12696.
(41) Imai, M.; Kaji, K.; Kanaya, T. *Phys. Rev. Lett.* **1993**, *71*, 4162; *Macromolecules* **1994**, *27*, 7103.
(42) Nogales, A.; Ezquerra, T. A.; Denchev, Z.; Baltá-Calleja, F. J. *Polymer* **2001**, *42*, 5711.
(43) Heintz, A. M.; McKiernan, R. L.; Gido, S. P.; Penelle, J.; Hsu, S. L.; Sasaki, S.; Takahara, A.; Kajiyama, T. *Macromolecules* **2002**, *35*, 3117.
(44) Imai, M.; Kaji, K. *Polymer* **2006**, *47*, 5544.

MA061188V